



## **FINITE ELEMENTS ANALYSIS OF INTERGRID BENDING TESTS ON USED FUEL RODS SAMPLES**

**Maurice DALLONGEVILLE**  
TN International (AREVA), France

**Aravinda ZEACHANDIRIN**  
TN International (AREVA), France

**Peter PURCELL**  
International Nuclear Services, U.K.

**Anthony CORY**  
International Nuclear Services, U.K.

### **ABSTRACT**

TN International and International Nuclear Services (INS) started in early 2000s a joint project, the Fuel Integrity Project (FIP), in order to develop a methodology to assess the response of Light Water Reactor (LWR) fuel assemblies (FA) during 9 meters regulatory drops. To this end, several series of mechanical tests were carried out on fresh and used fuel rods samples, including intergrid bending tests on samples of used fuel rods with average burn-up of 50 GW.d/tU.

In this framework, a preliminary analysis of the commissioning test (test 11.1) results was presented during Patram 2004; in complement, the analysis of the whole test series 11 (tests 11.1 to 11.6) is now presented.

The used test span matches a typical intergrid length of LWR FA. The load is applied at mid-span of the fuel rods samples by a pulley wheel. This test series leads to failures starting at a net lateral deflection of about 35 mm at room temperature and 60 mm at 500 °C, and with few percent high total elongations.

Calculation of the whole tests series was carried out with the ANSYS code using a shell and brick model. The different mechanical phenomena occurring during the tests were distinguished and the adequate fuel rods material parameters were determined.

The determination of these phenomena by preliminary calculations and the models validation were followed by a sensitivity study of the parameters values in the material constitutive laws to insure a good agreement between the obtained strength / deflection curves and the actual tests curves.

This sensitivity study was all the more efficient and reliable as the effects of each material parameter appeared almost sequentially and cumulatively during the loading of the fuel rods samples.

Even though models improvements might be possible, the guidelines of the retained approach lead to reference maximum elongations at rupture in consistency with literature values for used fuel rods.

The methodology to apply these Finite Element Analysis (FEA) results of bending test series 11 to an actual used FA during a 9 m lateral drop test is finally presented.

## INTRODUCTION

TN International and International Nuclear Services (INS) started in early 2000s a joint project, the Fuel Integrity Project (FIP), in order to develop a methodology to assess the response of Light Water Reactor (LWR) fuel assemblies (FA) during 9 meters regulatory drops. To this end, several series of mechanical tests were carried out on fresh and used fuel rods samples, including intergrid bending tests on samples of used fuel rods with average burn-up of 50 GW.d/tU.

In this framework, a test program and a preliminary analysis of the commissioning bending test (test 11.1) results were presented during Patram 2004 ([1] and [2]); in complement, the analysis of the whole bending test series 11 (tests 11.1 to 11.6), in which the used test span matches a typical intergrid length of LWR FA and the load is applied at mid-span of the fuel rods samples by a pulley wheel, is now presented.

The primary objective was to determine a reliable rupture (or non-rupture) limit by comparing calculations to actual tests curves. Additionally, it was also to propose an analytical approach (as part of FIP methodology) to apply this result to an actual used FA during a lateral drop test.

## REFERENCE TEST SERIES 11

The main input parameters of test series 11 are the PWR or BWR fuel types, the geometries, the Zr4 or Zr2 cladding materials, the average burn-up of 50 GW.d/tU, the levels of temperature (ambient or 500 °C) or pressure (atmospheric, 50 or 130 bars) and the existence of an initial preconditioning or not. The irradiated resisting sections of Table 1 were obtained by taking into account the in-reactor creep of pellets and cladding, and by subtracting the cladding oxide thickness. Some samples have been submitted to a preliminary axial impact at 1000 g (equivalent to actual 200 - 250 g on a full scale assembly) called “preconditioning”, which purpose is to increase pellets’ fragmentation.

Fuel pin type	Cladding outer diameter (mm)	Cladding thickness (mm)	Pellets outer diameter (mm)	Pellet length (mm)
PWR	10.65	0.585	9.48	15
BWR	10.65	0.70	9.25	11

**Table 1: Test series 11 resisting sections of irradiated samples at room temperature**

A first test device with a polyurethane pulley was used for the commissioning test 11.1, and a second one (especially developed) with a stainless steel pulley was used for the remaining five bending tests of series 11 (see Figure 1).

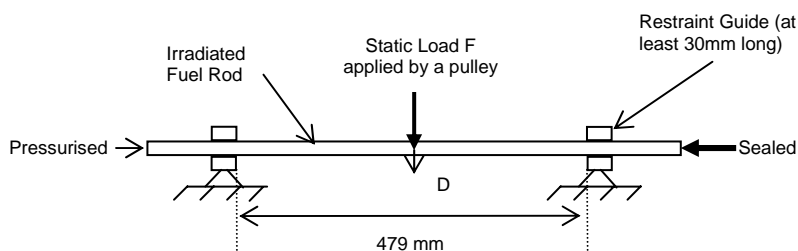


**Figure 1: Tests 11.2 to 11.6 device**

In both test devices, samples were positioned in guided supports and a pulley wheel applied a concentrated force at mid-span. For each test of series 11, the rupture appears on the lower part of the cladding at mid-span, just below the application point of the pulley wheel. A fuel collection tray was positioned below for fuel material release.

The strength / displacement tests curves (only up to first failure and smoothed to remove the Portevin-Le Chatelier indentations) are presented in Figure 2 in two groups with displacement shifts in relation to the two test temperatures (room temperature and 500 °C).

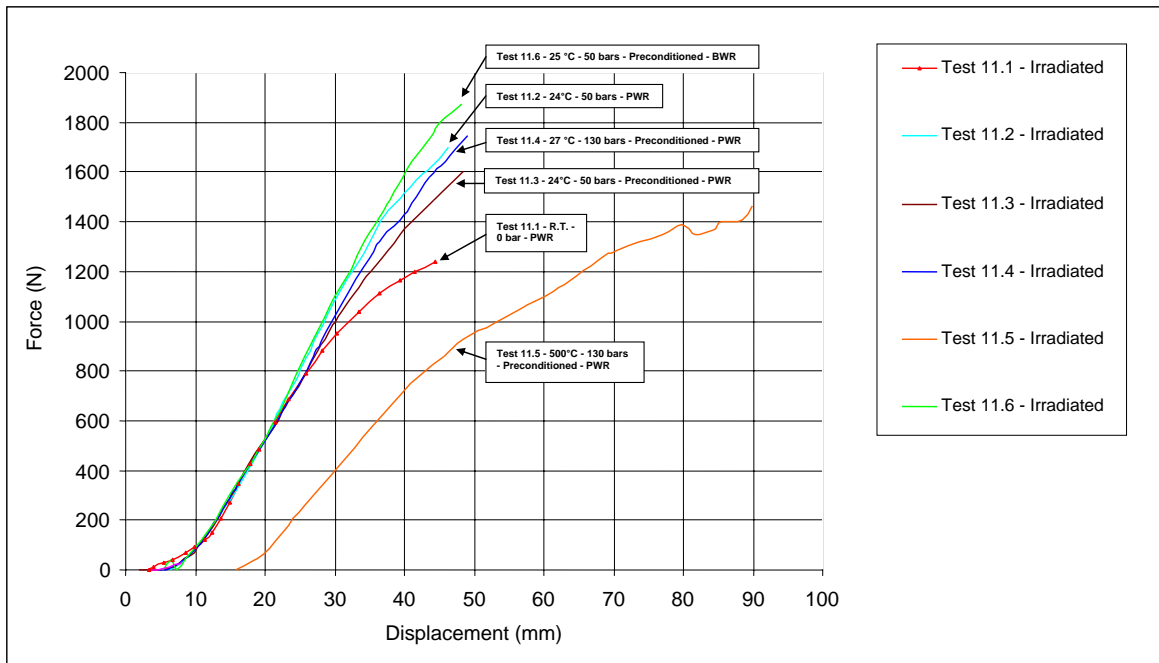


**Figure 2: Lateral bending tests series 11 - Smoothed curves**

## CALCULATION MODEL

The calculation of the whole tests series was carried out with the ANSYS code release 9.0 using a shell and brick model and a static approach (rate independent plasticity of material law - no viscosity effect) with elastic-plastic material law, large strain, large displacement or rotation, and stress stiffening.

### Fuel pin model

The numerical model used has the following characteristics: cladding is simulated using 3D shell elements; pellets, pulley wheel and support are simulated using 3D volume elements; contact is simulated by 3D surface-to-surface elements; screws are simulated using 3D uni-axial beam elements with tension, compression, torsion, and bending capabilities.

All elements (except contacts) are well suited for linear, large rotation, and / or large strain non-linear applications and include stress-stiffening terms. The FEA meshing has been optimised (symmetry conditions, bevelled edges at the supports / cladding contacts, specific pellets' modelling, etc...).

The loads are vertical mid-span load applied with the pulley wheel (3D solid element and surfacing contact element), and internal pressure. The boundary conditions of irradiated fuel pin are: symmetry conditions (a ¼ meshing is sufficient), contact conditions and friction coefficient between cladding and supports, friction coefficients between cladding, pellets and the various types of pellets parts.

The outer oxide layer of the cladding is considered having no mechanical strength. The pellets are completely bonded to the cladding. They are also fragmented with thermal radial cracks appeared in reactor and their tensile behaviour is not the same than the compressive one.

Two alternative models of pellets were studied:

- A simplified model: a homogeneous cylinder section is modelled along each pellet and is joined to the cladding. Axial discontinuity of pellets is respected.
- A complex model: a continuous thin layer stuck to the cladding and containing cylindrical quarters of one pellet length. Internal contacts are used between each pellet quarters. Axial discontinuity of the pellets quarters is respected.

#### Material constitutive laws

The cladding material constitutive law has a Voce form with constant asymptote:

- it is a linear elastic law, in relation to the Young modulus  $E_Y$ , up to the yield stress  $Re_z$ ,
- the plastic part of the curve is described by the following equation:

$$\sigma = Re_z + R_{Voce} \times \exp(-b_{Voce} \times \varepsilon_p),$$

- with :
- $\sigma$  : strength value, calculated from the material law,
  - $Re_z$ : Zircaloy cladding yield strength,
  - $R_{Voce}$  : range of potential strength increase due to the plastic deformations,
  - $b_{Voce}$  : inverse of a characteristic constant of the plastic deformations (determined from (un)irradiated zircaloy values),
  - $\varepsilon_p$  : plastic elongation of the cladding.

The used pellets' material constitutive law has an asymmetrical bilinear form and compressive values are actual, while tensile values are significantly lower in order to minimise unrealistic tensile effects (nevertheless, a minimal threshold permits to avoid numerical calculations instabilities).

No direct rupture criterion or modification of the material constitutive laws was used in the FEA to determine the cladding rupture; therefore, the calculation was only stopped at a displacement largely greater than the actual rupture level during the tests, and calculated parameters at first failure (or rupture) are further interpolated between values of the two neighbour nodes.

#### Principle of the calculations

The principle of the “inverse approach” used is to determine the parameters of the model directly from the observations and, if necessary, to search a more adapted model. It is carried out by making initial hypotheses on the form of phenomenon or model items as material constitutive laws or friction effects, and then optimising parameters values by iterative calculations to get acceptable matches of the pertinent parts of tests curves. The achievement of good matches by credible values of parameters validates the model.

The strength / deflection bending curves are calculated for the whole test series for several models and hypotheses and are compared to actual results curves. The resulting model is finally applied for each test of the test series 11.

Intergrid bending test curves present typically a first failure that is characterised by a first sudden strength decrease, and, after a further strength increase, a final rupture with a second sudden strength decrease and a complete opening of the whole rod section. These further strength variations have no direct interest and are not studied here.

## MODEL AND PARAMETERS OPTIMISATION

The model optimisation using the inverse approach was developed in progressive steps numbered from 0 to 5.

Step 0 - Choice of a pellet model on test 11.1 in consistency with the already known FEA results for this test [2]

Pellets yield strength in both models and the additional internal friction coefficient of the cracked pellet model were found to have a significant influence. Consequently, the cracked model is chosen, and applied in all following calculations in order to be more realistic than the simplified model.

The pressure was found having no significant influence in both models, which means also that it can be neglected for first approaches without loss of precision.

Step 1 - New analysis of test 11.1 with the cracked pellet model and complete modelling of the test device (checking of support beams deformation, not modelled previously)

The maximum stresses in the support beams were found lower than their yield strength indicating that the support beams (not modelled in previous 2004 study [2]) do not deform plastically. It is concluded that the support stiffness is sufficiently high to have no significant influence.

Step 2 - Elementary parametric analyses of test 11.1 and 11.2 with the cracked pellet model (extension at test 11.2)

The influence of the plastic parameters of cladding material constitutive law and of the cladding / support friction coefficient on the cracked model was first analysed on test 11.1. Test 11.2 was used after to extend the model as it is a typical room temperature (RT) case of the test series 11 carried out on the optimised device.

Zircaloy yield strength and, less significantly,  $b_{V_{oce}}$  parameter have some influence on the strength / displacement curve but  $R_{V_{oce}}$  parameter and pressure do not.

The influence of the friction coefficient at the support on the strength / displacement curve was found greater than the one of plastic parameters of the cladding material curves. However, modification of all these parameters leads to maximum relative discrepancy in strength with test 11.2 strength / displacement curve remaining high (about 15 %).

Step 3 - Global model optimisation on all PWR tests at RT (extension at tests 11.3 and 11.4)

Previous step 2 shows that yield strength  $Re_z$  and cladding friction coefficient  $\alpha_S$  at support points have both significant influences in calculation and could be optimised simultaneously to have a better global coherence in the whole study. The new optimisation of test 11.1 calculation is obtained with a  $\pm 1$  % margin for optimised low friction coefficient  $\alpha_S$  at the support and standard Zircaloy yield strength  $Re_z$ . The best calculation results of test 11.2 are now within a  $\pm 8.8$  % margin for other optimised  $Re_z$  and  $\alpha_S$  (see Figure 3). It is better than the previous results of about 15 %, but not really consistent and acceptable. Furthermore, general test curves shape is not exactly respected as test 11.2 to 11.4 and 11.6 results curves seem in fact to show an inflexion point at an intermediate strength level.

Step 3A - Global model optimisation on all PWR tests at RT (extension at tests 11.3 and 11.4; new friction hypothesis)

The step 3 final precision of the FEA / test match was not satisfactory and raised a supplementary hypothesis on the cladding / support friction coefficient in this supplementary step "3A".

Analysing tests 11.2 to 11.4 actual strength / displacement curves and comparing all previous calculation results, a new physical explanation was suggested: the curves differences between the two tests series (i.e. test 11.1 vs. tests 11.2 to 11.4) seem essentially due to a sudden and ultimate increase of the friction at supports. This friction variation happens on the second PWR series for intermediate strength levels specific to each of the test 11.2 to 11.4.

It could correspond to a blocking phenomenon of the fuel pin cladding in the supports due to local plastic collapse or to external end effects on the sample that prevents the cladding axial sliding at least on one side. It did not concern the commissioning test 11.1 that was carried out on the preliminary test device and permits good matching by FEA with a constant low friction coefficient at support.

All the calculation results obtained with two friction coefficients for tests 11.2, 11.3 and 11.4 are now within a  $\pm 2.4\%$  margin of the actual test results, which is fully acceptable (see Figure 4).

#### Step 4 - Global model optimisation on BWR tests at RT (extension at test 11.6)

The same matching method is used for BWR calculations as for PWR step 3A calculations of tests 11.2 to 11.4 and the cladding material was considered to be Zircaloy 4 instead of Zircaloy 2. It produced quite good calculation results with a  $\pm 2.0\%$  margin.

Differential comparison of PWR and BWR models was also done for the same standard values of Zircaloy yield strength and cladding / support friction coefficient  $\alpha_s$  and it gives a 6.8% variation of calculated elongation between the two cases. It is also close to the PWR / BWR relative strength difference in room temperature tests 11.4 and 11.6, and comes from the combination of differences in cladding inertia (stiffness) and pellet length.

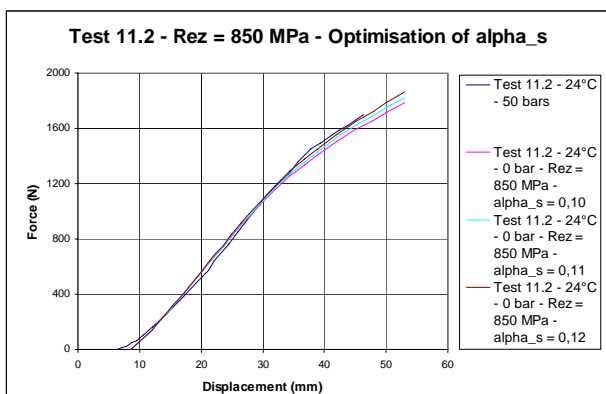


**Figure 3: Step 3 - Test 11.2 - First matching with Rez**

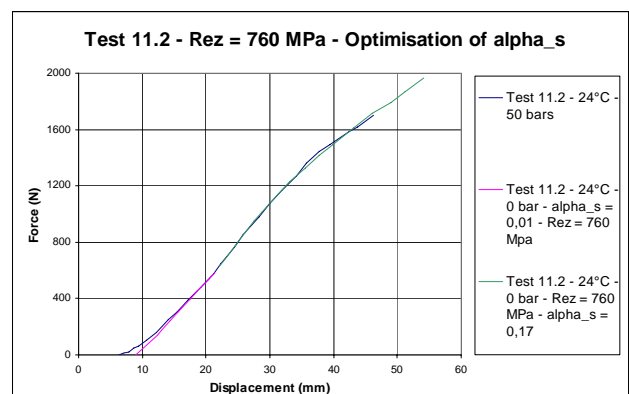


**Figure 4: Step 3A - Results for test 11.2 - Calculations without pressure**

#### Step 5 - Global model optimisation on PWR tests at 500 °C (extension at test 11.5)

Two successive calculation sub-steps of the bending test at 500 °C are done to solve the numerical divergence due to the gaps opening between pellets:

- A fuel pin thermal expansion is calculated first between room temperature and 500 °C.
- Internal pressure and load of the pulley wheel are applied secondly on the expanded model.

Calculation results obtained with a model using actual thermal expansion coefficients for both pellets and cladding are excessively unfavourable: stress levels are high and probably overestimated because the actual gaps between pellets, and between pellets and cladding, are not taken into

account. Therefore, in the remaining part of the study, the cladding thermal expansion coefficient is applied to fragmented pellets because the cladding limits their expansion.

A sudden change in the cladding / support friction coefficient (actual or equivalent) has been also necessary, as for calculation of tests 11.2 to 11.4 and test 11.6, to obtain a rather good matching in temperature with a  $\pm 4.7\%$  margin between FEA and test curves (see Figure 5). This matching could be improved slightly if some further small variations of the friction coefficient  $\alpha_s$  were considered between 65 and 80 mm.

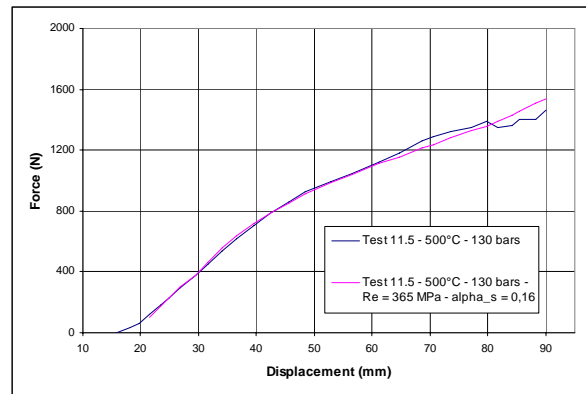


**Figure 5: Step 5 - Test 11.5 Strength / Displacement**

## FINAL RESULTS

The final results obtained in steps 3A to 5 of previous sections have been updated, when necessary, to take into account internal pressure measured in tests. As expected, it does not modify significantly the strength / displacement calculation results previously obtained. Typical calculated curves of other parameters are presented for test 11.2 in Figures 6 to 8. The calculation global precision is indicated on Table 2. The net bending deflections and maximum elongations at rupture are presented on Table 3.

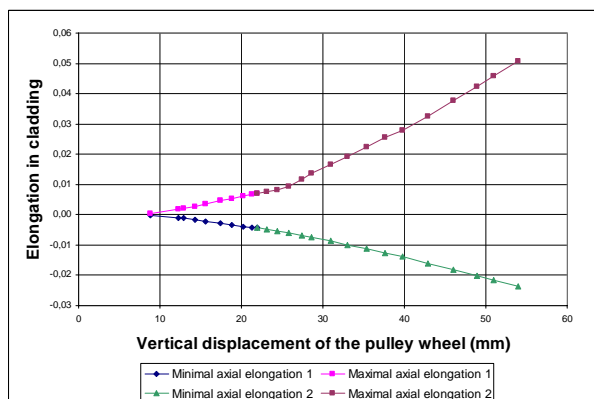


**Figure 6: Test 11.2 - Cladding axial elongations (outer diameter of top layer)**

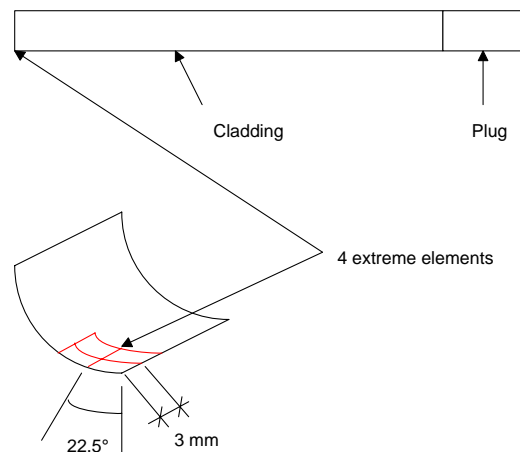


**Figure 7: Test 11.2 - Location of the 4 elements for local axial elongation**

Pellets' modelling in quarters induces local stress concentrations in claddings span; hence maximum elongations are not fully reliable to establish a cladding rupture criterion. Nevertheless, as elongations obtained at mid-span in the symmetry plane and / or at the supports are not much concerned by stress concentrations, they permit to establish cladding rupture limits. This is explained by a lower pellets / cladding relative shearing due to the symmetry of the system that is reflected in the boundary conditions.

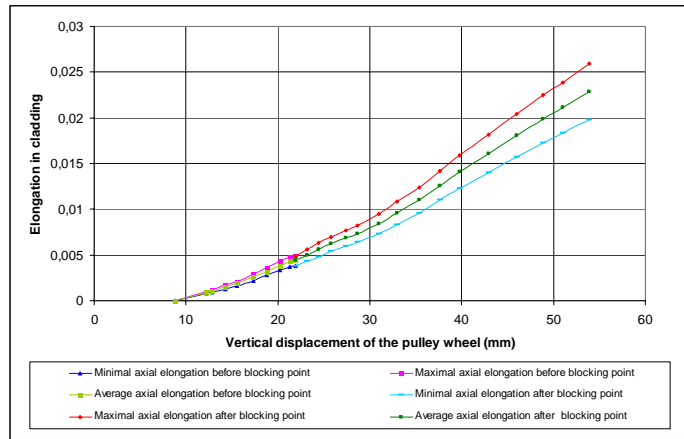


**Figure 8: Test 11.2 - Local axial elongation in symmetry plane (top layer)**

The FEA results for test 11.5 at 500 °C show obviously that the elongation on extreme fibre is a more stable and reliable value (total elongation rupture is about 2 to 3 %) to establish a rupture criterion than the maximum global elongation with pellets local effects that can give non realistic high values (about 20 %) due to the discontinuous aspect of pellets modelling in calculations.

Test case	11.1	11.2	11.3	11.4	11.5	11.6
First $\alpha_s$	0.01	0.01	0.01	0.01	0.01	0.01
Second $\alpha_s$	-	0.17	0.11	0.16	0.16	0.17
Transition strength (N)	-	600	750	750	300	600
Transition shift (mm)	-	0.74	1.56	1.26	1.20	1.31
Global precision	$\pm 1 \%$	$\pm 2.4 \%$	$\pm 2.0 \%$	$\pm 1.6 \%$	$\pm 4.7 \%$	$\pm 2.4 \%$

**Table 2: Final optimised friction considerations and global precision**

Temperature (°C)	Test number	Net bending deformation (mm)	Maximum elongation in symmetry plane (%)	Maximum global elongation (%)
Room temperature	20	Test 11.1	35.56	1.80
	24	Test 11.2	37.46	<b>2.06</b>
	24	Test 11.3	39.78	2.13
	27	Test 11.4	40.44	2.21
	25	Test 11.6	39.41	2.14
High temperature	500	Test 11.5 (fail.)	61.91	<b>2.28</b>
	500	Test 11.5 (rupt.)	72.16	2.60
				20.17

NB: The theoretical elongation at yield is 0.78 % at room temperature and 0.53 % at 500 °C.

**Table 3: FIP irradiated tests 11.1 to 11.6 - Synthesis of cladding rupture elongations**

The reference elongations at the cladding top layer that are retained as conservative rupture limits for the methodology are the 2.1 % at room temperature (test results from the second device) and 2.3 % at 500 °C values at mid-span in the symmetry plane (or at the supports) as they correspond to pure cladding bending and axial elongation. They are reliable and consistent with the temperature and depend neither on pellets modelling, nor on the stress concentrations they induce. Furthermore, they are consistent with the purely axial elongation value of the cladding top layer calculated by mechanical analytical formulas and similar to the values in the literature [3].

## RESULTING METHODOLOGY

The test series 11 consisted in LWR fuel rods samples loaded at mid-span with a concentrated force and sliding guides at each end, while rods in assemblies are uniformly loaded on each intergrid in lateral drop and their boundary conditions are defined by the type of fuel assembly and the



considered intergrid location. The case temperatures are generally different from the two temperature levels tested (i.e. 24 and 500 °C).

The application of the reference rupture deformations, from the reference tests to a studied lateral drop case, is developed by taking into account, step-by-step, the differences in temperature, geometry, material, boundary conditions and load with the drop case. If necessary, rupture elongations for other irradiation levels than the reference 50 GW.d/tU from tests can be estimated using irradiated material laws.

The methodology is mainly built on the consideration of the equality of the axial elongations at rupture of irradiated rods at similar temperature and irradiation. Elastic beam deformation profile is taken into account in the displacement formula to simplify the model in order to solve it by simple mechanical formulas. Due to the uniform load distribution of the fuel pin during assemblies' lateral drop, potential ruptures of an actual fuel pin preferentially occur at supports levels and not at mid-span.

The shifting of the reference rupture deformations, from the reference tests to a studied axial drop case can also be developed on the basis of the above approach, considering an additional step taking into account boundary conditions specific to Euler buckling. In consistency with boundary conditions, the possible rods' ruptures by Euler buckling in axial drop occur at mid-span of the bottom intergrid zone and not at rods ends.

## **CONCLUSION**

An inverse approach of the test series 11 results has been carried out by FEA in several progressive steps of model optimisation by search of internal parameters minimising the discrepancies in strength / displacement curves. It has permitted better understanding of the involved physical parameters (friction and material law coefficients) and brought information on the fragmented pellets behaviour, as well as on the sudden increase of the friction coefficient at supports, which appeared systematically on tests 11.2 to 11.6 carried out on the second test device and led to a model modification.

Even though improvements of FEA bending models might still be possible, the guidelines of the retained approach for used fuel pins behaviour analysis in lateral drop lead, after analysis, to conservative reference cladding elongations at rupture in consistency with literature values.

A simple methodology to shift the irradiated cladding deformation at rupture obtained by Finite Element Analysis from bending test series 11 to the loading of an actual used FA during 9 m lateral or axial drop tests has been developed to predict the occurrence of fuel rods bending rupture.

## **REFERENCES**

- [1] "Fuel Integrity Project: Testing of LWR Fuel Rods to Support Criticality Safety Analysis of Transport Accident Conditions" Patram 2004 - Peter C Purcell from BNFL International Transport, Spent Fuel Services - Maurice Dallongeville from COGEMA LOGISTICS (AREVA Group) -
- [2] "Fuel Integrity Project: Analysis of Light Water Reactor Fuel Rods Test Results" Patram 2004 - Maurice Dallongeville, Jürgen Werle from COGEMA LOGISTICS (AREVA Group) - Gerard McCreesh from BNFL Nuclear Sciences and Technology Services
- [3] "Mechanical properties for irradiated Zircaloy", Transactions of the American Nuclear Society ISSN 0003-018X - 2005, vol. 93, p. 707-708 - Academic Press, New York, NY, États-Unis (1958), J. Kenneth; E. Beyer Carl